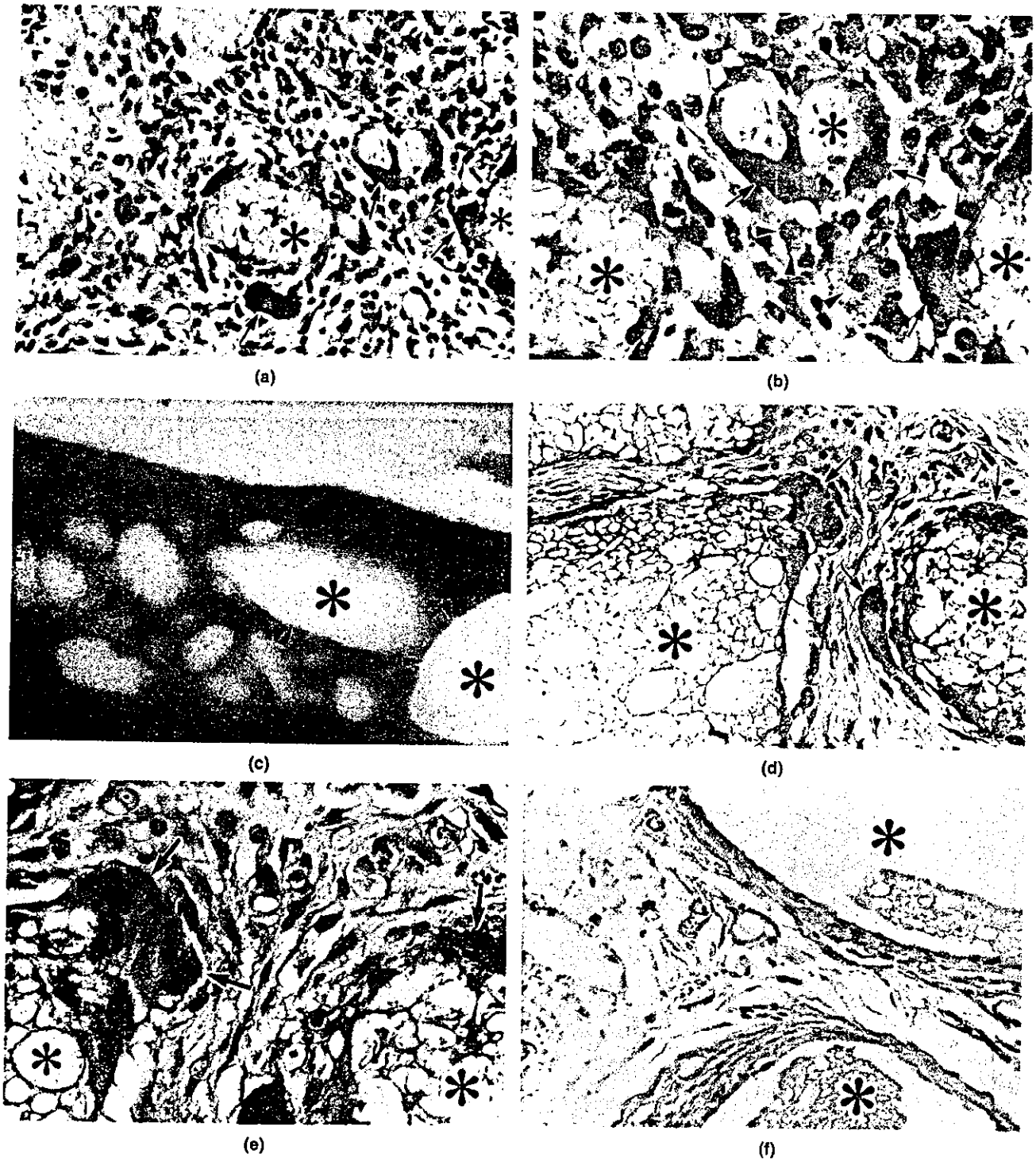

Figure 3. Soft tissue response to the control cement. (a) Moderate inflammation and numerous foreign body giant cells (arrow) are seen around the crumbled control cement (*) at 1 week after surgery. Hematoxylin and eosin stain: original magnification ×100. (b) High magnification of (a). Foreign body giant cells (arrow) can be seen on the surface of the cement (*). Macrophages (arrowhead) are seen in the granulation tissue around the crumbled cement (*). Hematoxylin and eosin stain: original magnification ×200. (c) Calcein (arrowhead) injected at surgery is deposited on the surface of the crumbled control cement (*) at 2 weeks. Fluorescent microscopy: original magnification ×25. (d) Many foreign body giant cells (arrow) can be observed on the surface of the crumbled control cements (*) at 4 weeks. Hematoxylin and eosin stain: original magnification ×100. (e) High magnification of (d). Foreign body giant cells (arrow) are seen on the surface of the cement (*). Mesenchymal cells and fibroblasts can be seen in the fibrous tissue. H.E. stain: original magnification ×200. (f) Crumbled cement pieces (*) are covered by thin connective tissue with fibroblasts at 26 weeks. Hematoxylin and eosin stain: original magnification ×100.

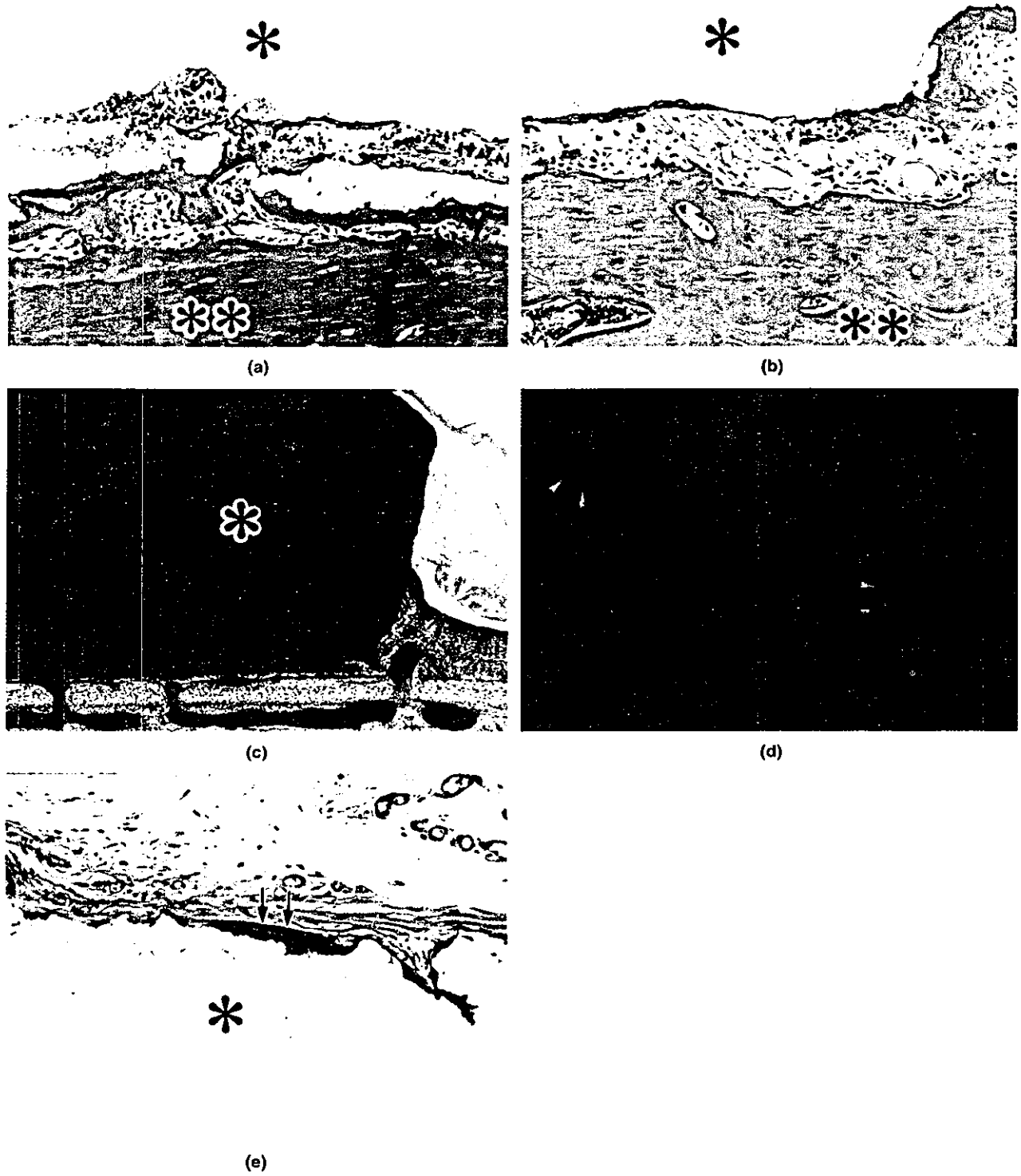

Figure 4. Hard tissue response to the new cement. (a) New bone formation can be observed in the gap between the host parietal bone (**) and the new cement (*) at 2 weeks. Hematoxylin and eosin stain: original magnification ×50. (b) Thin new bone can be observed on the under surface of the new cement (*) detached from host parietal bone (**) at 4 weeks. Hematoxylin and eosin stain: original magnification ×50. (c) Most of the edge and under surface of the new cement (*) is covered by newly formed bone at 8 weeks. Villanueva bone stain: original magnification ×10. (d) Calcein (arrow) deposition can be seen on the surface and alizarine complexone (arrowhead) deposition is seen on the inner layer of the new cement at 8 weeks. Fluorescent microscopy: original magnification ×10. (e) Slight bone formation (arrow) can be observed on the upper surface of the new cement (*) at 52 weeks. Hematoxylin and eosin stain: original magnification ×50.

face of the cement at 52 weeks [Fig. 4(e)]. There were no multinuclear cells on the surface of the cement. Distinct cell-mediated absorption of the cement was not observed.

Control cement group

At 1 week after surgery, the periosteum covering the cement was thickened with a prominent inflammatory response. The cement crumbled to pieces, and small pieces were covered by granulation tissue with an inflammatory response. Although newly formed bone directly contacted some of the small pieces of the cement on the host parietal bone, many of the pieces of cement were covered by fibrous connective tissue with an inflammatory response at 2 weeks [Fig. 5(a,b)]. At 4 weeks after surgery, although some of the small pieces contacted the new bone directly, most were covered by fibrous connective tissue and granulation tissue [Fig. 5(c)]. At 8 weeks, some particles of the control cement were contacted with newly formed bone and foreign body giant cells were observed on the surface of the particles covered by fibrous connective tissue [Fig. 5(d)]. Even at 26 weeks after surgery, foreign body giant cells were observed on the control cement particles covered by fibrous connective tissue [Fig. 5(e)].

XRD analysis

Figure 6 shows the XRD patterns of the new cement and the control cement implanted in subcutaneous tissue. At 1 day after surgery, peaks of HAP were observed for both cements and peaks of DCPD were slightly detected, whereas some peaks of TeCP and relatively high peaks of TCP remained. At 1 week after surgery, the intensity of peaks of HAP was increased in both cements. Small peaks assigned to TCP and TeCP were observed in the new cement, and a quite small peak of TCP was observed in the control cement. At 8 weeks, both cements had been transformed to HAP. Figure 7 shows the changes of the rates of transformation to HAP. The rates increased with time with both cements. The components of the cement were completely transformed to HAP by 8 weeks after surgery. The rate of transformation of the control cement was higher than that of the new cement at every measuring point.

FT-IR analysis

Figure 8 shows the FTIR spectra of the new cement and the control cement implanted in the subcutaneous tissue. The peak at 1560 cm^{-1}, which was detected for calcium succinate but not for the original powder, was considered to be derived from chelation. This peak was detected in new cement and it decreased with the time of implantation.

DISCUSSION

The cement reported in the present study was a calcium phosphate cement containing carboxylic acid. The liquid components of calcium phosphate cement reported in many studies were distilled water or neutral phosphate solution.[5–8,10–13] We studied calcium phosphate cement containing a carboxylic acid and a polysaccharide. Carboxylic acid is thought to chelate calcium of the powder components and strengthen the mechanical properties, shorten the setting time and make an insoluble matrix as a result.[19] In contrast, it was reported that organic acid causes an inflammatory response.[9,20] One shortcoming of the calcium phosphate cement containing carboxylic acid was surplus acid that did not take part in the chelation reaction. We previously developed a calcium phosphate cement containing citric acid and chitosan and reported that the content of citric acid in the liquid component was related to the extent of inflammation around the cement.[14] We then changed citric acid to succinic acid to reduce the inflammatory response. The cement caused a moderate inflammatory response when implanted in putty form and a slight inflammatory response when implanted in prehardened form.[15] In this study, the content of succinc acid was reduced from 8.0% to 3.9%. Inflammation at the early implantation stage was slight despite the use of the putty form, whereas surplus acid was recognized in an *in vitro* study.[16,17] Therefore, the control of inflammation could be accomplished by decreasing the content of succinic acid.

Moderate inflammatory and foreign body responses were observed around the control cement, whereas slight inflammatory changes and only a few foreign body giant cells were observed around the new cement. Miyamoto et al. reported severe inflammation around calcium phosphate cement implanted immediately after mixing.[21] They proposed that the severe inflammation was the result of a decrease of transformation to HAP and the crumbling of the cement. Takechi et al. reported that calcium phosphate cement without citric acid crumbled and that a severe inflammatory response was observed when it was implanted immediately after mixing, whereas calcium phosphate cement with citric acid did not crumble and there was little inflammatory change.[20] In this study, the transformation rate of the control cement was higher than that of the new cement despite the moderate inflammation. A moderate inflammatory reaction was recog-

Figure 5. Hard tissue response to the control cement. (a) Some of the crumbled cement pieces (*) are covered by new bone from the host parietal bone (**). An inflammatory response can be seen around the crumbled cement at 2 weeks. Hematoxylin and eosin stain: original magnification ×50. (b) High magnification of (a). Some cement pieces (*) are covered by new bone. Many foreign body giant cells (arrow) are seen on the surface of the crumbled cement. Hematoxylin and eosin stain: original magnification ×100. (c) Some of the crumbled cement pieces (*) are covered by bone tissue. Other crumbled cement particles (**) are covered by fibrous connective tissue at 4 weeks. Hematoxylin and eosin stain: original magnification ×50. (d) Some cement pieces (*) are covered by bone. Foreign body giant cells (arrow) can be seen on the surface of the cement pieces surrounded by thin fibrous connective tissue at 8 weeks. Hematoxylin and eosin stain: original magnification ×50. (e) A foreign body giant cell (arrow) can be seen on the surface of the cement (*) in the fibrous tissue at 26 weeks. Hematoxylin and eosin stain: original magnification ×100.

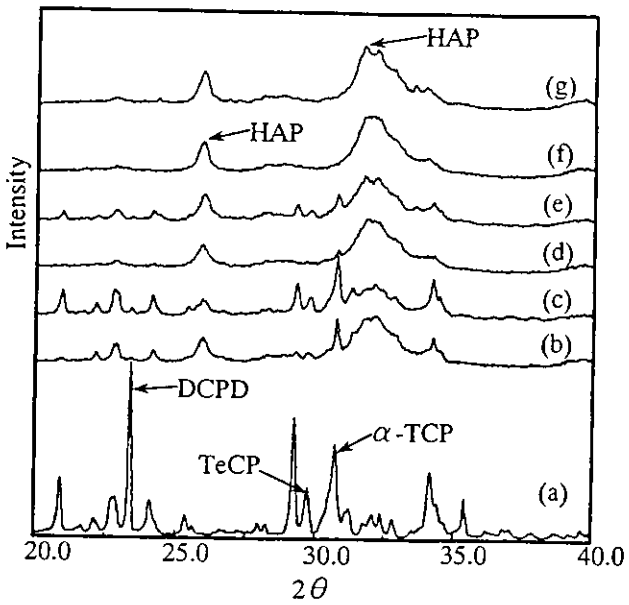

Figure 6. XRD patterns of the cements implanted in the subcutaneous tissue. (a) original powder; (b) the control cement at 1 day; (c) the new cement at 1 day; (d) the control cement at 1 week; (e) the new cement at 1 week; (f) the control cement at 8 weeks; and (g) the new cement at 8 weeks.

nized where only cement powder (average diameter 22 μm) was implanted in our preliminary study. Therefore, the crumbling of the cement was thought to be the main reason for the inflammatory response of the control cement. There have been some reports on the relation between the particle size of the material and the extent of inflammatory reaction.[22,23] The crumbling of the control cement seemed to be due to low mechanical strength and the inhibition of the interlocking of HAP crystals by the penetration of blood, as reported by Ishikawa et al.[11] In contrast, an insoluble matrix was formed by chelation in the new cement, so the mechanical strength increased and the penetration of blood, which resulted in crumbling, did not occur. Therefore, it was thought that the inflam-

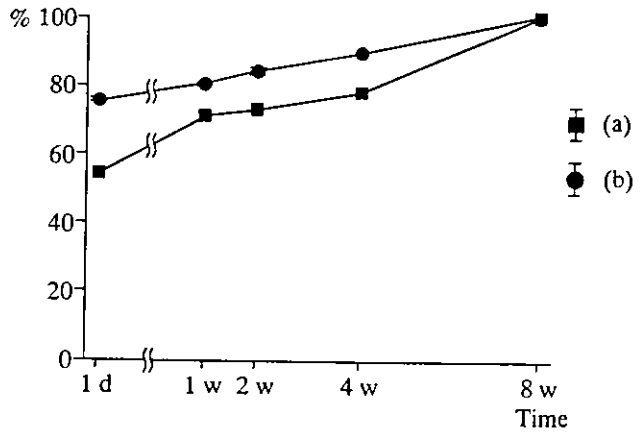

Figure 7. Transformation rate to HAP in the subcutaneous tissue. (a) the new cement; (b) the control cement.

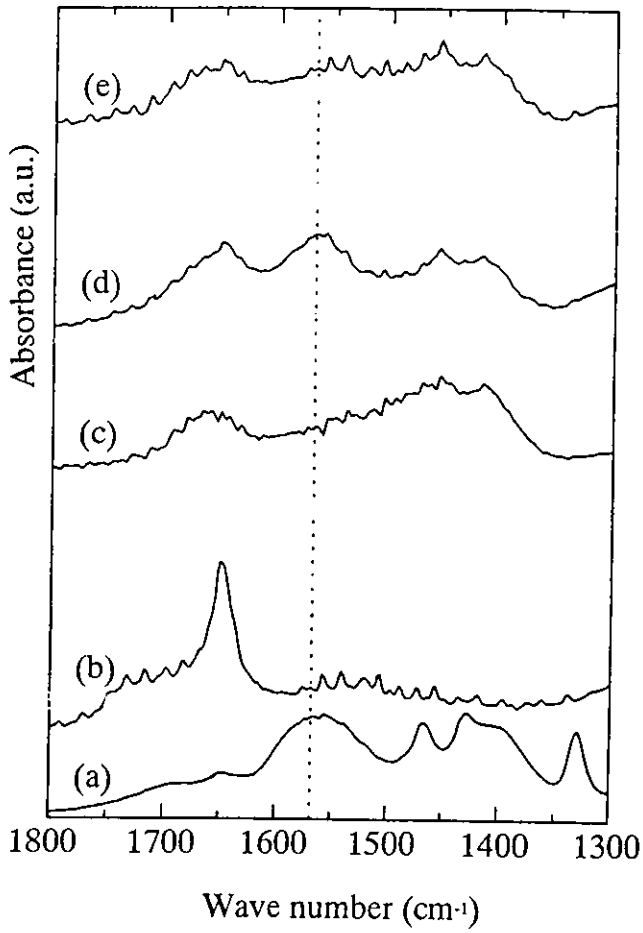

Figure 8. FT-IR spectra of the cements implanted in the subcutaneous tissue. (a) calcium succinate; (b) original powder; (c) the control cement at 1 week; (d) the new cement at 1 week; and (e) the new cement at 8 weeks.

matory response around this new calcium phosphate cement was related to surplus acid and that around the control cement was related to the fragmented cement particles. In fact, there was little inflammatory response around prehardened control cement that did not crumble.[15] When this control cement is used, it should be used in prehardened form or in conditions without blood penetration. On the other, because the insoluble matrix formed by chelation inhibited hydration, transformation to HAP occurred later than with the control cement.

The biocompatibility and osteoconductivity of calcium phosphate cement have been reported in several studies.[7,24–29] For osteoconductivity, it has been reported that the components and setting reaction products of calcium phosphate cements are the main inorganic constituents of hard tissue.[28] The new cement showed good osteoconductivity in this study, as thin new bone was directly formed on the surface of the new cement detached from the host parietal bone. Good fitting to the host bone is also considered to be related to osteoconductivity. Poor fitting of the material to the host bone, as with the block form of HAP,

could cause penetration of fibrous tissue and bone resorption under the material. Because the new cement fit to the parietal bone, the resorption of the host bone was not observed. Fitting is believed to be related to the fixation of the material. Donath et al. reported that the initial stability of the implanted material was important for osteoconductivity.[30] The implanted control cement immediately crumbled, thus fixation of the cement was not sufficient, and there were inflammatory responses around the pieces of the cement. Therefore, osteoconduction of the control cement was less than that of the new cement, although some of pieces of the control cement close to the host bone were covered by new bone. Furthermore, calcium deposits were observed on the new cement from immediately after surgery. This might have been related to the increase in the calcium ion concentration around the cement that accompanied the dissolution of the cement by the surplus acid. Calcium deposition on the surface of the cement in the early implantation stage would be effective for osteogenesis around the cement. CM-chitin, which was added the new cement to improve its handling properties, has been studied as a drug carrier.[31] It was also reported that calcification was promoted on it.[32]

The resorption of calcium phosphate cement has been controversial. Miyamoto et al. implanted fast-setting calcium phosphate cement in bone defects made on rat tibiae and reported that no resorption of the cement was observed within 8 weeks.[24] Kurashina et al. implanted calcium phosphate cement onto the cranial bone of the rabbit and reported that differences of the surrounding tissue resulted in different resorption rates.[25] Frankenburg et al. implanted injectable calcium phosphate cement into proximal tibial metaphyseal and distal femoral metaphyseal defects in dogs and reported that the mean percentage of the cavity occupied by the cement had decreased to 34.1% in the tibial defects and 67% in the femoral defects at 78 weeks.[26] Ikenaga et al. implanted calcium phosphate hydraulic cement into bone cavities created in the distal epiphysis of femurs in rabbits, and reported the cement was resorbed, leaving only 7.67% after 12 weeks.[27] In a clinical study, Sarkar et al. reported the partial replacement of their calcium phosphate cement by new bone.[29] The differences in the rates of resorption were considered to be related to the differences of the compositions and properties of the cements, and the species and ages of the animals. However, most of these studies showed that osteoclasts were related to resorption of cement. Yuan et al. implanted calcium phosphate cement into the femoral bone of the dog for 6 months. They reported that the calcium phosphate cement was resorbed by chemical dissolution and cell-mediated resorption.[28] In this study, distinct cell-mediated resorption of either the control or newly developed cement in the subcutaneous tissue and on the bone was not observed within 12 months. Few macrophages and foreign body giant cells were observed on the surfaces of the cements at 12 months, although they were observed at the early implantation stage. Observation by fluorescent microscopy revealed that calcium deposition occurred not only on the surface but also in the inner area of the new cement with time. In vitro study showed dissolution of the new cement in physiologial saline even at 4 weeks after immersion.[17] In addition, the decrease of the chelation of the calcium succinicate in the new cement detected by FTIR showed the dissolution of calcium succinate. These results suggested that calcium was deposited in the void via the dissolution of calcium succinate. Although the quantity was very small, when the above results are considered, only chemical dissolution of the cement seems to have been occurred.

In conclusion, our newly developed calcium phosphate cement containing succinic acid and CM-chitin showed excellent biocompatibility and osteocompatibility over a long period of time. However, it will be necessary to carry out further experimental research to validate its clinical use in the future.

References

1. Jarcho M. Calcium phosphate ceramics as hard tissue prosthetics. Clin Orthop 1981;157:259–278.
2. Kent JN, Finger IM, Quinn JH, Guerra LR. Hydroxyapatite alveolar ridge reconstraction: clinical experience, complications and technical modifications. J Oral Maxilofac Surg 1986; 44:37–49.
3. Wittkampf ARM. Augmentation of the maxillary alveolar ridge with hydroxylapatite and fibrin glue. J Oral Maxillofac Surg 1988;46:1019–1021.
4. Hupp JR, Mckenna S. Use of porous hydroxylapatite blocks for augmentation of atrophic mandibles. J Oral Maxillofac Surg 1988;46:538–545.
5. Monma H, Kanazawa T. The hydration of α-tricalcium phosphate. J Ceram Soc Jpn 1976;84:209–213.
6. Brown WE, Chow LC. Combinations of sparingly soluble calcium phosphates in slurries and paste as mineralizers and cements. US Patent 4,612,053, 1986.
7. Hong YC, Wang JT, Hong CY, Brown WE, Chow LC. The periapical tissue reactions to a calcium phosphate cement in the teeth of monkeys. J Biomed Mater Res 1991;25:485–498.
8. Bermudez O, Boltong MG, Driessens FCM, Planell JA. Development of some calcium phosphate cements from combinations of α-TCP, MCPM and CaO. J Mater Sci Mater Med 1994; 5:160–163.
9. Kurashina K, Kurita H, Hirano M, de Blieck JMA, Klein CPAT, de Groot K. Calcium phosphate cement: in vitro and in vivo studies of the α-tricalcium phosphate-dicalcium phosphate dibasic-tetracalcium phosphate monoxide system. J Mater Sci Mater Med 1995;6:340–347.
10. Ishikawa K, Takagi S, Chow LC, Ishikawa Y. Properties and mechanisms of fast-setting calcium phosphate cements. J Mater Sci Mater Med 1995;6:528–533.
11. Ishikawa K, Miyamoto Y, Kon M, Nagayama M, Asaoka K. Non-decay type fast-setting calcium phosphate cement: composite with sodium alginate. Biomaterials 1995;16:527–532.
12. Constantz BR, Ison IC, Fulmer MT, Poser RD, Smith ST, Van-

Wagoner M, Ross J, Goldstein SA, Jupiter JB, Rosenthal DI. Skeletal repair by in situ formation of the mineral phase of bone. Science 1995;267:1796–1799.
13. Friedman CD, Costantino PD, Takagi S, Chow LC. BoneSource™ Hydroxyapatite Cement: A novel biomaterial for craniofacial skeletal tissue engineering and reconstruction. J Biomed Mater Res (Appl Biomater) 1998;43:428–432.
14. Yokoyama A, Kamiura Y, Takahashi R, Shigeno K, Yamamoto S, Takeishi A, Komatsubara H, Kawasaki T, Kohgo T, Amemiya A. Experimental study of self hardening hydroxyapatite for bone substitute material. J Dent Res 1994;73:914.
15. Yokoyama A, Yamamoto S, Komatsubara H, Takeishi A, Kawasaki T, Kohgo T, Nakasu M. Development of calcium phosphate cement containing carboxymethyl-chitin and succinic acid for bone substitute. J Jpn Prosthodont Soc 2000;44:9–18.
16. Yokoyama A, Yamamoto S, Fujita R, Matsuno H, Ohori K, Komatsubara H, Takeishi A, Iida S, Sasoh F, Kawasaki T, Kohgo T. Self-hardening hydroxyapatite using succinic acid for a bone substitute material. J Dent Res 1999;78:410.
17. Nakasu M, Matsushima A, Ogawa T, Yokoyama A, Tajima M, Hukuhara T. Mechanical properties of calcium phosphate cement containing CM-chitin and succinic acid. Biomaterials; submitted for publication.
18. Fukase Y, Eanes ED, Takagi S, Chow LC, Brown WE. Setting reactions and compressive strengths of calcium phosphate cements. J Dent Res 1990;69:1852–1856.
19. Monma H. Materials chemistry of calcium phosphate cement. J Jp Soc Biomaterials 1997;15:24–30.
20. Takechi M, Miyamoto Y, Ishikawa K, Toh T, Yuasa T, Nagayama M, Suzuki K. Initial histological evaluation of anti-washout type fast-setting calcium phosphate cement following subcutaneous implantation. Biomaterials 1998;19:2057–2063.
21. Miyamoto Y, Ishikawa K, Takechi M, Toh T, Yuasa T, Nagayama M, Suzuki K. Histological and compositional evaluations of three types of calcium phosphate cements when implanted in subcutaneous tissue immediately after mixing. J Biomed Mater Res (Appl Biomater) 1999;48:36–42.
22. Goodman SB, Fornasier VL, Lee J, Kei J. The histological effects of the implantation of different sizes of polyethylene particles in the rabbit tibia. J Biomed Mater Res 1990;24:517–524.
23. Sjögren U, Sundqvist G, Nair PN. Tissue reaction to guttapercha particles of various sizes when implanted subcutaneously in guinea pigs. Eur J Oral Sci 1995;103:313–321.
24. Miyamoto Y, Ishikawa K, Takeuchi M, Toh T, Yoshida Y, Nagayama M, Kon M, Asaoka K. Tissue response to fast-setting calcium phosphate cement in bone. J Biomed Mater Res 1997;37:457–464.
25. Kurashina K, Kurita H, Kotani A, Kobayashi S, Kyoshima K, Hirano M. Experimental cranioplasty and skeltal augmentation using an α-tricalcium phosphate/dicalcium phosphate dibasic/tetracalcium phosphate monoxide cement: preliminary short-term experiment in rabbits. Biomaterials 1998;19:701–706.
26. Frankenburg EP, Goldstein SA, Bauer TW, Harris SA, Poser RD.Biomechanical and histological evaluation of calcium phosphate cement. J Bone and Joint Surg. 1998;80-A:1112–1124.
27. Ikenaga M, Hardouin P, Lemaitre J, Andrianjatovo H, Flautre B. Biomechanical characterization of a biodegradable calcium phosophate hydraulic cement: A comparison with porous biphasic calcium phosphate ceramics. J Biomed Mater Res 1998; 40:139–144.
28. Yuan H, Li Y, de Bruijin JD, de Groot K, Zhang X. Tissue responses of calcium phosphate cement: a study in dogs. Biomaterials 2000;21:1283–1290.
29. Sarkar MR, Wachter N, Patka P, Kinzl L. First histological observations on the incorporation of a novel calcium phosphate bone substitute material in human cancellous bone. J Biomed Mater Res (Appl Biomater) 2001;58:329–334.
30. Donath K, Rohrer MD, Hörmann K. Mobile and immobile hydroxyapatite integration and resorption and its influence on bone. J Oral Implantol. 1987;13:120–127.
31. Watanabe K, Sakai I, Uraki Y, Tokura S, Azuma I. 6-o-carboxymethyl-chitin (CM-chitin) as a drug carrier. Chem Pharm Bull (Tokyo) 1990;38:506–509.
32. Wan AC, Khor E, Wong JM, Hastings GW. Promotion of calcification on carboxymethyl chitin discs. Biomaterials. 1996;17: 1529–1534.

生体材料(デンタルインプラント)を目的とした傾斜機能材料の作製と生体反応

横山敦郎[*1]／川崎貴生[*2]／亘理文夫[*3]

1．はじめに

(1) デンタルインプラントとは？

厚生労働省の歯科疾患実態調査によると60歳の人の欠損歯数は10.45歯であり，70歳では16.61歯と著しく増加する[1]．歯牙欠損は，咀嚼や発音などのさまざまな機能障害をもたらし，今後到来する超高齢化社会においては，高齢者のQOLの低下が危惧される．このような歯の欠損に対する処置として，少数歯欠損に対しては残存歯にセメントで合着する固定性の補綴装置であるブリッジが，多数歯欠損に対しては可撤性の補綴装置である有床義歯が選択されることが，これまでは一般的であった．近年，歯の欠損に対する処置として，デンタルインプラント(人工歯根)に関する多くの基礎的および臨床的研究がなされ，広く臨床に普及されつつある[2,3]．従来のブリッジや義歯を用いた処置に比較し，人工歯根は残存歯を切削することがないため齲蝕を継発する危険性が少なく，また義歯に比較し，小さく，固定性であるため異物感が小さく，咀嚼機能も優れているという利点を持つが，インプラント埋入に十分な骨量および骨質が必要であること，顎骨に埋入するという外科処置が必要であること，さらには高価であることなどの問題点もある．

[*1] Atsuro Yokoyama 北海道大学病院咬合系歯科 講師 歯学博士
[*2] Takao Kawasaki 北海道大学大学院歯学研究科 口腔機能学講座 教授 歯学博士
[*3] Fumio Watari 北海道大学大学院歯学研究科 口腔健康学講座 教授 工学博士
Fabrication and Investigation of Tissue Reaction of Functionally Graded Implant for Biomaterial.

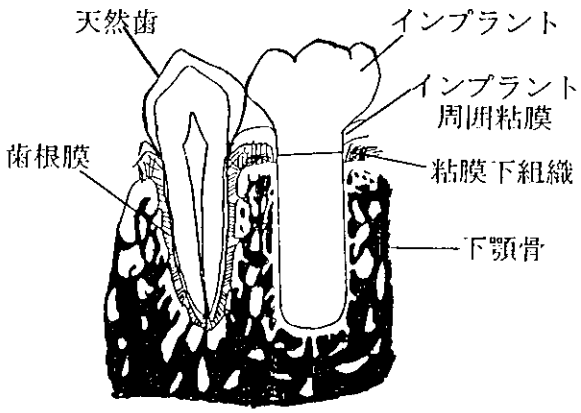

図1 下顎骨，天然歯およびデンタルインプラント模式図

図1に下顎骨，天然歯およびデンタルインプラントの模式図を示す．顎骨は，表層近くの皮質骨およびその内側の海綿骨から構成され，表層の皮質骨から内層の海綿骨へは，傾斜的に構造が緻密な状態から粗な状態となっており，圧を受けるのに適した構造となっている．天然歯は歯根膜を介し，顎骨の一部である歯槽骨に位置している．歯根膜には，感染防御，感覚認知および緩衝など機能があり，理想的にはこの歯根膜組織を有するデンタルインプラントの開発が望まれるが，現在使用されているデンタルインプラントには，天然歯根に見られる歯根膜組織がなく，光学顕微鏡的には，直接骨と接している．このようなインプラントと骨組織の接触状態は，オッセオインテグレーションと定義されている[1]．

(2) デンタルインプラントへの傾斜機能材料の応用

デンタルインプラントの材質に関しては，チタ

ン，チタン合金が主であり，さまざまな表面処理が施されている[5]．これらの表面処理は，オッセオインテグレーションを促進し，より強固なインプラントと骨組織との結合を目的としており，現在も多くの表面処理に関する研究が行われている．しかし，臨床で使用されているデンタルインプラントや研究されているインプラントの多くは，表面処理の有無は別として単一の材料からなっている．インプラントは，図1に示すように口腔内において，骨組織，粘膜下組織および口腔粘膜と接し，さらに骨組織は部位により構造が異なることから，インプラントにおいても部位により組成が異なる構造が力学的にも生物学的にも望ましい．明確な界面を持たず徐々に組成が変化する傾斜機能材料は，当初は「超高温構造材料の熱応力緩和」を目的に開発された材料であるが，この特性は，生体材料としても優れていると考えられている．われわれは，このような背景に基づき，部位により最適な機械的強度と生体適合性を有するデンタルインプラントを開発するため，傾斜機能材料の概念を応用した(図2)[6,7]．

2．傾斜機能型デンタルインプラントの開発

(1) CIP-電気炉加熱による傾斜機能型インプラント

原材料として機械的強度に優れ，生体適合性にも優れるチタン(Ti)粉末と骨適合性および伝導性に優れるセラミックスであるハイドロキシアパタイト(HA)粉末を用いた．これらの粉末を長さ方向に，Ti 100%から Ti 80%/HA 20%になるよう濃度勾配をつけた後，冷間静水圧(CIP)装置を用いて加圧し，電気炉にて焼結して作製した Ti/HA 系傾斜機能型インプラントの機械的性質および生体反応を観察した[8,9]．Ti，HA ともに骨組織との適合性に優れることから，作製した傾斜機能材料は良好な生体適合性を示し，Ti 粉末のみを同様の方法により焼結した Ti 材に比較し多くの骨組織が観察された(図3)．しかし，組成を変化させることにより組織の反応が傾斜することは確認されなかった．このため，Ti に比較し生体適合性に劣るコバルト(Co)を用いて，一端が Ti 100%，他端が Co 100%の傾斜構造を有するインプラントを作製し，ラットの皮下組織に埋入した．埋入2週後の所見として，Ti 側では材料表面に菲薄な線維性結合組織が観察されたが，Co 側方向に向かい線維性結合組織は肥厚し，組織内の炎症性細胞数が増加し，試料表面の一部の組織は変

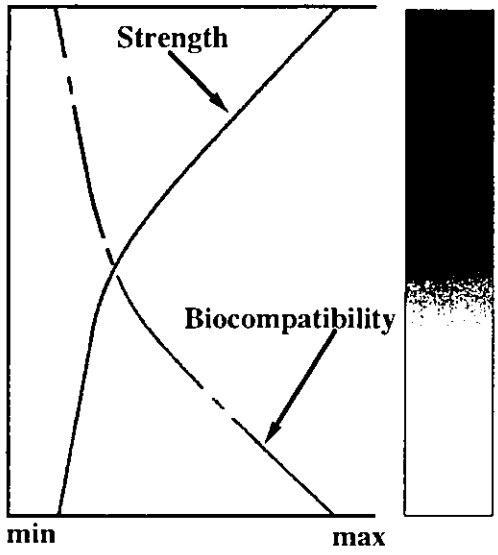

図2　傾斜機能型デンタルインプラントの概念模式図

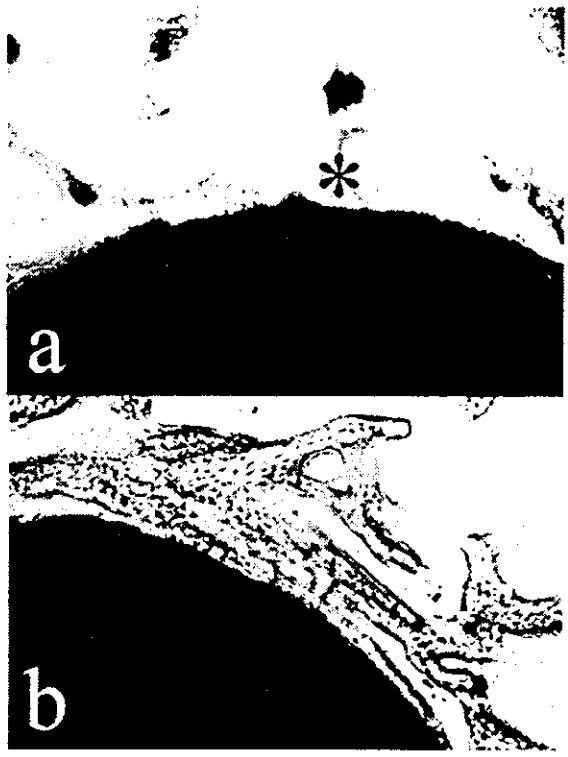

図3　CIP-電気炉加熱による傾斜機能型インプラント周囲の組織像
a：Ti 材，b：傾斜機能型インプラント Ti 80%/HA 20%側．a に比較し，b の新生骨は多い．ラット下顎骨埋入4週後．＊：新生骨（佐相史徳，横山敦郎，亘理文夫，川崎貴生．北海道歯誌，18：85-104（1997)より引用）

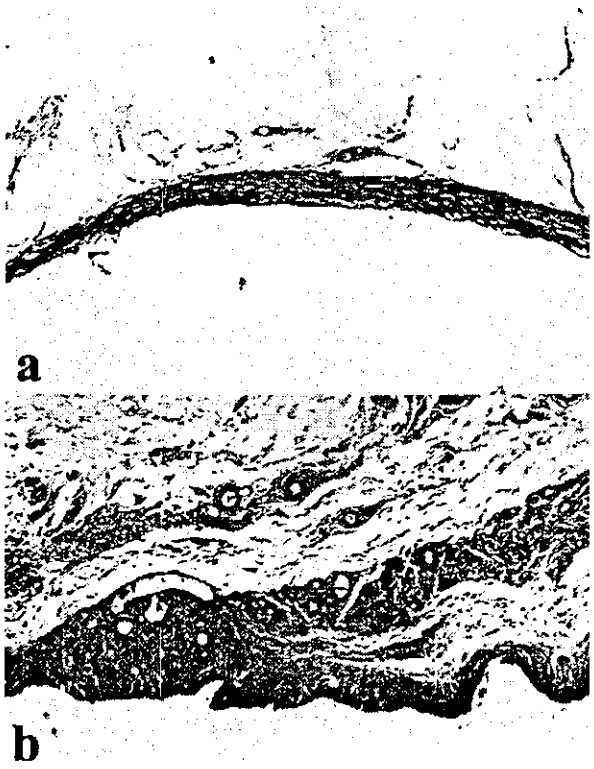

図4　Ti-Co 傾斜機能型インプラント周囲の組織像
a：Ti 側，b：Co 側．Ti 側には薄層の線維性結合組織が観察されるが，Co 側には炎症性細胞浸潤が結合組織内に認められる．ラット腹部皮下埋入 2 週後

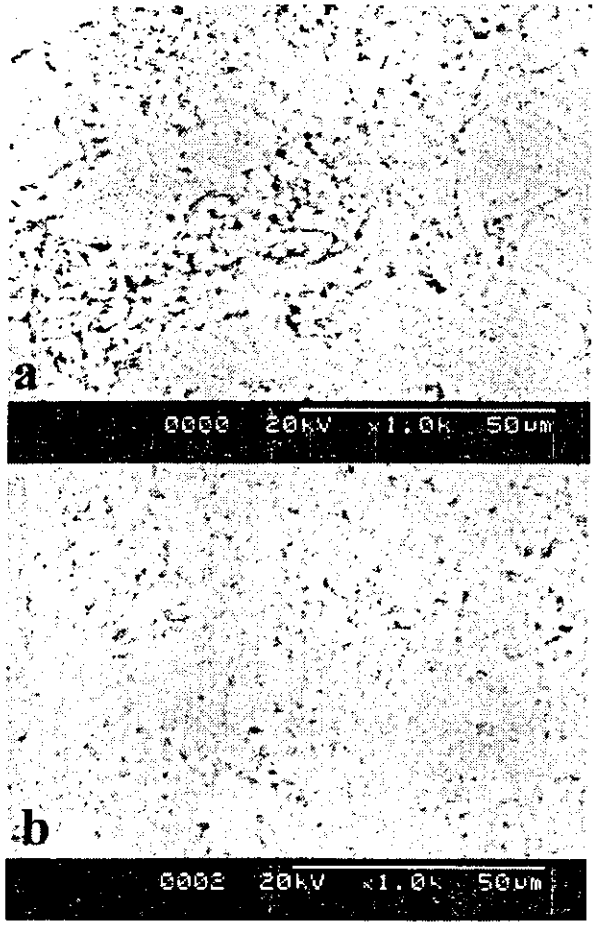

図5　CIP-電気炉加熱法および SPS 法にて作製した Ti-HA 複合体の SEM 像
a：CIP-電気炉加熱法，b：SPS 法．b は a に比較し焼結性に優れ緻密である（Yokoyama, A., Watari, F., Miyao, R. *et al. Bioceramics*, 13：445-448（2000）より引用）

性していた（図 4）．これは，材料の組成を傾斜させることにより，生体組織の反応を傾斜させる可能性を示唆しており，この結果から，Ti と HA の傾斜範囲を拡大することにより骨組織の反応を傾斜させることが可能ではないかという考えに至った．

(2) SPS(Spark Plasma Sintering)法を用いたチタン-ハイドロキシアパタイト複合体

CIP-電気炉加熱による傾斜機能型インプラントは，焼結不足と HA の高温での分解反応のため，安定して作製可能な濃度傾斜の範囲は Ti～20% HA（Ti 100%～80%）までであった[9]．これを解決するため，SPS 法に着目した．SPS 焼結装置では，圧粉体粒子間隙に発生したプラズマの高エネルギーを熱拡散することにより，粉体表面でのプラズマが粒子間に拡散するため，圧粉体全体の均一な焼結を促進し，効率の良い焼結が可能となる[10]．このため，金属およびセラミックスのいずれの焼結にも有効な方法といえる．予備実験として，複合比を変えた水素化 Ti-HA 複合体（Ti-HA 複合体）を放電プラズマ焼結装置で，焼結温度 1150℃，40MPa で加圧し，作製した[11]．SPS 法にて作製した Ti-HA 複合体は，CIP-電気炉加熱で作製したものに比較し，焼結性に優れ緻密であった（図 5）．また，組織学的には，HA と水素化 Ti の複合比に応じて，材料表面に形成される骨組織に変化が見られた．すなわち，埋入 8 週後では，20%Ti-80%HA においては，50%Ti-50%HA より骨組織の量は少ないが材料表面との接触は多く，改造も進んでいることが明らかとなった（図 6）．この結果から，SPS 法で作製した HA-Ti 複合体は，複合比を変化させることによりインプラント周囲の骨組織の量ならびに性状を制御できる可能性が示唆され，SPS 法にて HA/Ti 傾斜機能型インプラント作製することとした[12]．

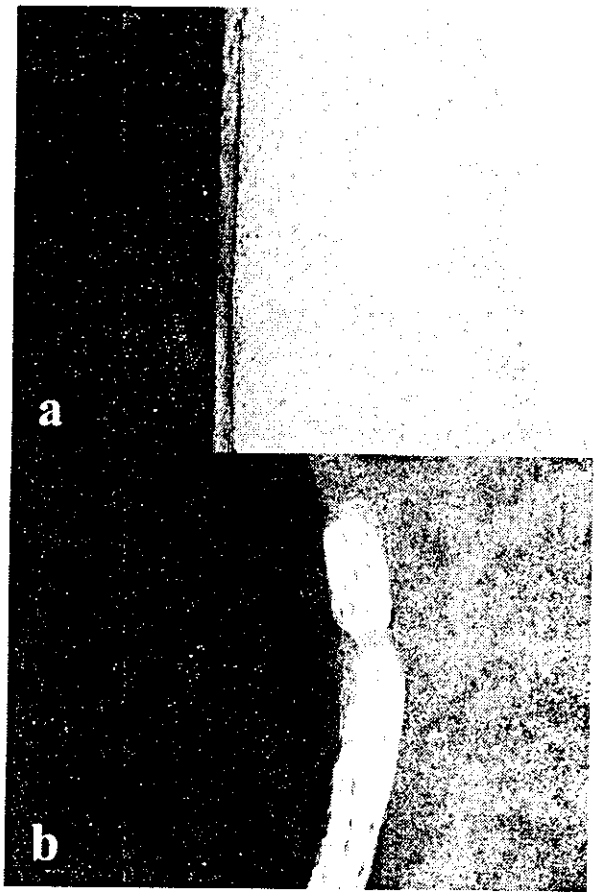

図6　SPS法にて作製したTi-HA複合体の組織像
a：20%Ti-80%HA，b：50%Ti-50%HA．aの表面の骨組織はbに比較し，改造が進み菲薄である(Yokoyama, A., Watari, F., Miyao, R. *et al. Bioceramics*, **13**：445-448 (2000)より引用)

(3) SPS法を用いたHA/Ti傾斜機能型インプラント

原材料として，微粉を除去した水素化Ti粉末(粒径44μm以下)と1150℃で焼結後粉砕し得られたHAの粉末(粒径45μm以下)を使用し，これら粉末を種々の割合で混合し，濃度勾配ができるようグラファイト製モールドに充填し，焼結温度および加圧条件を変化させ，放電プラズマ焼結装置で焼結した[13,14]．焼結温度は，HAの分解を抑える温度に設定したが，1000～1300℃においては内部応力の解放や局所的な高温還元状態によるHAの分解により，また750～800℃では焼結不足により，試料は崩壊し，焼結温度850℃，加圧条件40MPaおよび80MPaの条件下においてのみ，Ti 100%からHA 100%までの傾斜機能型インプラントが作製可能であった[14]．この条件で作製したインプラントについて，X線分析顕微鏡

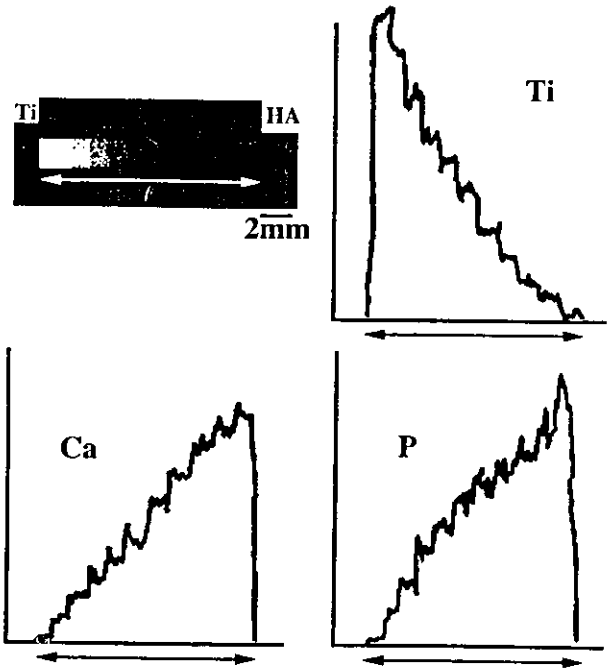

図7　Ti/HA傾斜機能型インプラントのX-SAMによるTiマッピング像と長軸方向の元素分布解析(宮尾里香，横山敦郎，亘理文夫，川崎貴生，歯科材料・器械，20：344-355 (2001)より引用)

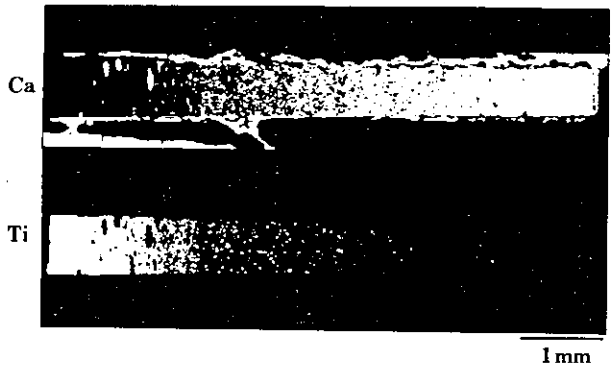

図8　埋入8週後のTi/HA傾斜機能型インプラント周囲のEPMAマッピング像(宮尾里香，横山敦郎，亘理文夫，川崎貴生，歯科材料・器械，20：344-355 (2001)より引用)

(X-SAM)，走査型電子顕微鏡(SEM)および電子線プローブマイクロアナライザー(EPMA)を用いて表面を分析するとともに，物性および生体適合性について検索した．X-SAMにて，TiとHAの構成成分であるCaおよびPのX線強度は連続的に変化し，TiとHAが，濃度傾斜していることが明らかとなり，動物埋入後の試料のEPMAによる面分析においても同様に濃度傾斜が確認された(図7，8)．SEM観察にて，焼結圧が高いほうがHAの多い部分においても緻密であるこ

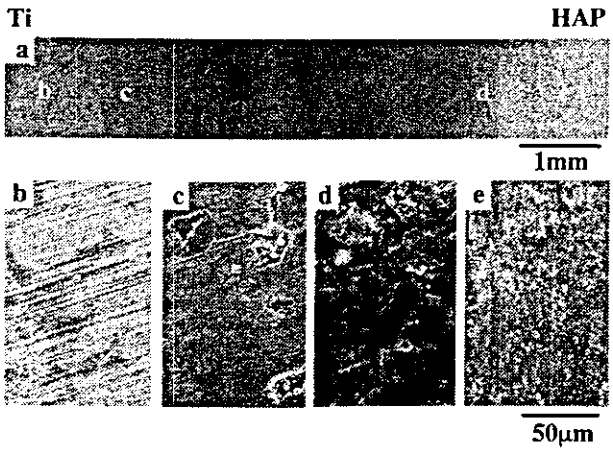

図9　焼結圧力80MPaで焼結したTi/HA傾斜機能型インプラントのSEM像 a：全体像，b～e：各部の拡大像(宮尾里香，横山敦郎，亘理文夫，川崎貴生，歯科材料・器械，20：344-355（2001)より引用)

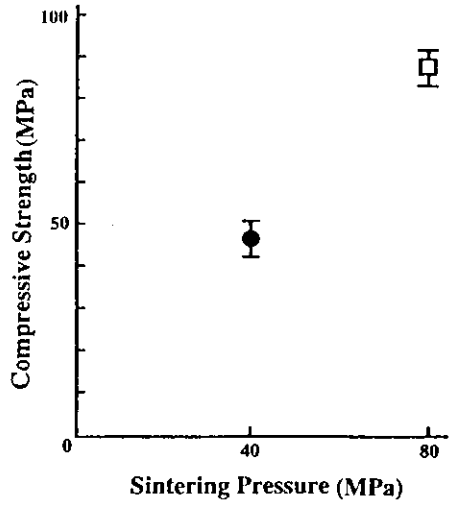

図10　Ti/HA傾斜機能型インプラントの圧縮強さのSPS焼結圧依存性(宮尾里香，横山敦郎，亘理文夫，川崎貴生，歯科材料・器械，20：344-355（2001)より引用)

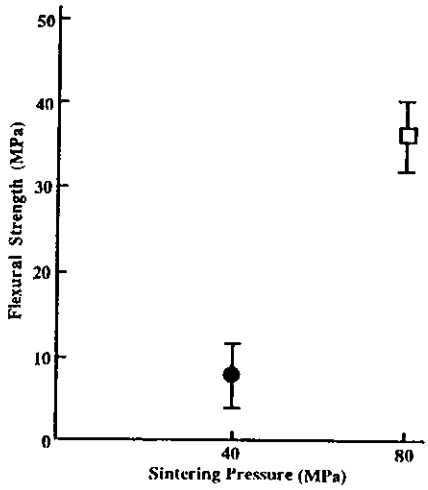

図11　Ti/HA傾斜機能型インプラントの3点曲げ強さのSPS焼結圧依存性(宮尾里香，横山敦郎，亘理文夫，川崎貴生，歯科材料・器械，20：344-355（2001)より引用)

とが示された(図9)．圧縮強さと3点曲げ試験の結果を図10および図11に示す．焼結圧80MPaで作製したもののほうが，40MPaで作製したものに比較し，圧縮強さは約2倍，3点曲げ強さは約5倍の値を示した．また，3点曲げ試験における破断は，40MPaの場合は試料の中心よりHA側で生じたが，80MPaでは試料のほぼ中央で生じた．これは，焼結圧の高いほうが，焼結性が向上し緻密になったためと推察される．ラット大腿骨への埋入試験において，埋入4週後ではHAが多い部分に幼若な新生骨が観察され，8週では新生骨組織は増加したが，特にHAが多い部分では試料と骨との接触率は高い傾向を示した．埋入16週においては，試料と骨組織との接触は，Ti，HAともにさらに増加していたが，図12に示すように，Tiが多い部分の新生骨は細胞成分が多く比較的幼若な像を呈していたが，HAが多い部分の新生骨は，改造が進み，菲薄化し層板構造を呈していた．この結果は，TiをHAコーティングしたインプラントとTiインプラントの骨形成を比較し，HAコーティングしたほうが初期の骨接触率は高いが，長期経過後はTiのほうが高いとした報告と同様であり[15]，前述のSPS法を用いた種々の複合比のTi-HA複合体を埋入した結果を同一の試料に集約したものといえる．これらのことから，Ti/HA傾斜機能型インプラントの使用は，同一の試料で部位により異なった組織の反応を生じ，組成の傾斜に応じて生体，特に骨組織の反応を制御できる可能性が示唆された．

3．今後の展望

これまでに，SPS装置を用いることにより，小型のTi/HA傾斜機能型インプラントを作製し，組成の傾斜に応じた組織反応の傾斜を生じさせることが可能となった．現在，機械的強度および焼結性の向上およびHAの分解の抑制のため，水素化Tiの代わりに窒化Tiの使用を試み，良好な結果を得ている[16]．今後は，物性の向上を図るとともに，臨床での応用を目的とした大型動物を用いた咬合力を負荷する動物実験をすすめていく予定である．

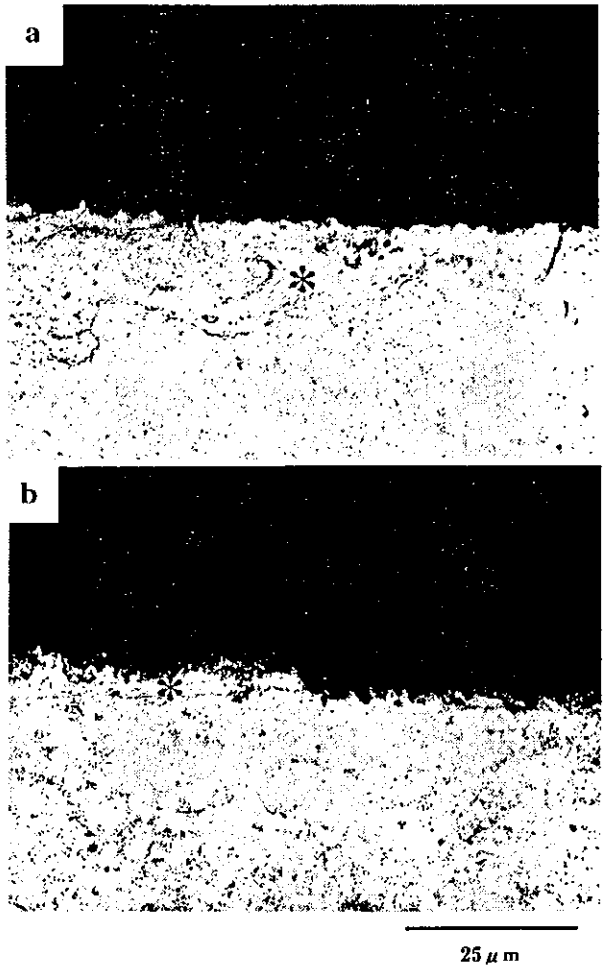

図12 Ti-HA傾斜機能型インプラント周囲の組織像
a：Ti高濃度部，b：HA高濃度部．aには細胞の多い比較的幼若な骨組織が観察されるが，bの骨組織は，改造が進み菲薄である．＊：新生骨(宮尾里香，横山敦郎，亘理文夫，川崎貴生，歯科材料・器械，20：344-355 (2001)より引用)

謝　辞

本論文に記載した多くの研究を行った宮尾(田村)里香博士，佐相史徳博士，近藤英臣大学院生また研究に協力していただきました宇尾基弘助教授，松野浩宜博士，田村豊博士に感謝いたします．試料の作製に際し，多大なご協力を戴きました東北大学金属材料研究所平井敏雄名誉教授，大森守助手，大久保昭技官に深謝いたします．また，本研究の一部は平成8年度科学研究費補助金重点領域研究「傾斜機能材料の物理・化学」および平成10～12年度科学研究費補助金基盤研究A10307049の補助により行った．

文　献

1) 2000年度版歯科保険関係統計資料－口腔保険・歯科医療の統計－，厚生省健康政策局歯科保健課，口腔保健協会 (2000)
2) Gotfredsen, K., Wennerberg, A., Johansson, C., Teil Skovgaard, L., Hjorting Hansen, E : Anchorage to TiO_2-blasted, HA-coated and machined implants, An experimental study with rabbits. *J. Biomed. Mater. Res.*, **37** : 60-67 (1997)
3) Lindquist, LW., Carlsson, GE., Jemt T. A prospective 15-year follow up study of mandibular fixed prostheses supported by osseointegrated implants clinical results and marginal bone loss. *Clin. Oral Imp. Res.*, **7** : 329-336 (1996)
4) Brånemark, P-I. : Introduction to Osseointegration in clinical dentistry. Brånemark,P-I., Zarb, G.A. and Albrektsson, T. (ed.). Quintessence Pub. Co., Inc., Chicago, 11-76 (1985)
5) 塙　隆夫，生体用金属材料の表面処理とその効果，表面技術，**43**：739-743 (1992)
6) 高橋秀直，歯科用傾斜機能材料の研究－チタン-アパタイト，チタン-ジルコニア傾斜材の強度特性－，歯科材料・器械，**12**：595-612 (1993)
7) 亘理文夫，傾斜機能人工歯根，セラミックス，**29**：191-193 (1994)
8) Watari, F., Yokoyama, A., Saso, F., Uo, M., Kawasaki, T. Fabrication and properties of functionally graded dental implants, *Composites Part B*, **28B** : 5-11 (1997)
9) 佐相史徳，横山敦郎，亘理文夫，川崎貴生，チタン/ハイドロキシアパタイト系傾斜機能型インプラントの作製と生体親和性に関する研究，北海道歯誌，**18**：85-104 (1997)
10) 鴇田正雄，放電プラズマ焼結(SPS)システムの現状と将来性，住友石炭鉱業，1-14 (1995)
11) Yokoyama, A., Watari, F., Miyao, R., Matsuno, H., Uo, M., Kawasaki, T., Kohgo, T., Omori, M., Hirai, T. Mechanical properties and biocompatibility of titanium-hydroxyapatite implant material prepared by spark plasma sintering method, *Bioceramics*, **13** : 445-448 (2000)
12) 大森　守，大久保　昭，宮尾里香，亘理文夫，平井敏雄，SPS法によるチタニウム/ハイドロキシアパタイト系傾斜機能材料の作製，粉体および粉末冶金，**47**：1234-1238 (2000)
13) 宮尾里香，大森　守，亘理文夫，横山敦郎，松野浩宜，平井敏雄，川崎貴生，放電プラズマ法による傾斜機能型インプラントの試作と特性，粉体および粉末冶金，**47**：1239-1242 (2000)
14) 宮尾里香，横山敦郎，亘理文夫，川崎貴生，放電プラズマ焼結法で作製したチタン/アパタイト系傾斜機能型インプラントの特性と生体反応，歯科材料・器械，**20**：344-355 (2001)
15) Gottlander, M., Albrektsson, T., Carlsosn, LV. A histomorphometric study of unthreaded hydroxyapatite-coated and titanium-coated implants in rabbit bone, *Int. J. Oral Maxillofac Implants*, **7** : 485-490 (1992)
16) 近藤英臣，横山敦郎，川崎貴生，宇尾基弘，大川昭治，菅原　敏，赤坂　司，亘理文夫，放電プラズマ焼結法で作製した窒化チタン/アパタイト系傾斜機能型インプラントの物性と生体適合性の評価，歯科材料・器械，**22(S)**：54 (2003)

Materials Transactions, Vol. 45, No. 11 (2004) pp. 3156 to 3162

Fabrication of Titanium Nitride/Apatite Functionally Graded Implants by Spark Plasma Sintering

Hideomi Kondo[1], Atsuro Yokoyama[1], Mamoru Omori[3], Akira Ohkubo[3], Toshio Hirai[4], Fumio Watari[2], Motohiro Uo[2] and Takao Kawasaki[1]

[1]*Removable Prosthodontics and Stomatognathostatic Rehabilitation, Department of Oral Functional Science, Graduate School of Dental Medicine, Hokkaido University, Sapporo 060-8586, Japan*
[2]*Dental Materials and Engineering, Department of Oral Health Science, Graduate School of Dental Medicine, Hokkaido University, Sapporo 060-8586, Japan*
[3]*Institute for Materials Research, Tohoku University, Sendai 980-8577, Japan*
[4]*Japan Fine Ceramics Center, Atsuta, Nagoya 456-8587, Japan*

Titanium nitride/hydroxyapatite functionally graded implant (TiN/HAP) was successfully fabricated by spark plasma sintering method (SPS) and their properties were investigated. The functionally graded materials (FGM) with the concentration from TiN at one end to HAP at the other were prepared by sintering at 1100 and 1200°C under the pressure of 150 MPa. The Brinell hardness was around H_B 60, nearly uniform for the whole range of composition. After 2 and 8 week implantation in diaphysis of femur of rat, there was very little inflammation and the new bone was formed around the sample. By use of TiN instead of Ti, the decomposition of HAP during sintering process could be suppressed and the successful sintering of FGM and mechanical properties could be attained.

(Received July 21, 2004; Accepted September 2, 2004)

Keywords: *titanium nitride, hydroxyapatite, functionally graded materials, spark plasma sintering, implant, biocompatibility*

1. Introduction

Pure titanium, titanium alloys, and hydroxyapatite are used for the implant in dental clinics as the method to restore the mastication function of lost teeth. Hydroxyapatite (HAP), a main component of bone and teeth, has bioactive properties for new bone formation.[1-3] Most of these implants are composed of the same structure and materials for the whole part. The dental implant needs the different function from part to part since it penetrates into a jawbone from the inside of the mouth. Inside the bone, the implant material is required to have osseoconductivity so that the new bone can be formed quickly and attached directly to it (osseointegration). In oral cavity (outside the bone), the implant material is required to have enough mechanical strength to bear the occlusal force. However, most of dental implants have the uniform composition throughout from the upper to bottom. The implant receives the force as much as 600 N at occlusion, nearly about the patient's weight. Inside jaw bone, the uniform fixation of the implant by new bone formation which completely surrounds the whole surface of implant is desirable to have the sufficient strength endurable to the occlusal force and to have the stress relaxation effect, that is, release of the excess overload on jaw bone. Dental implant with functionally graded structure would satisfy these requirements, high bone affinity and relaxation effect. Thus, we have been developing the dental implant where the concept of a functionally graded material (FGM) was applied. Figure 1 shows the concept of FGM implant. As a typical example, the left end is 100%Ti and the right end is 100%HAP. If Ti content increases, mechanical properties would be improved and as HAP content increases, biocompatibility could be improved.

Titanium/hydroxyapatite functionally graded implant (Ti/HAP) has thus been developed using pure titanium, titanium hydride, and surface nitrided titanium as the starting titanium materials for sintering.[4-16] However, HAP becomes unstable and decomposed under the coexistence of Ti which tends to act as reductant at high temperature. In Ti/HAP, the compromised optimum sintering temperature was found as 850°C where HAP is not decomposed.[15] However, at this temperature, sintering and mechanical intensity was insufficient. The use of more inert material, titanium nitride (TiN), would suppress the decomposition of HAP and enable the sintering at higher temperature. In this study, the TiN/HAP functionally graded implant was fabricated by Spark Plasma Sintering (SPS) and its mechanical properties and biocompatibility were investigated.

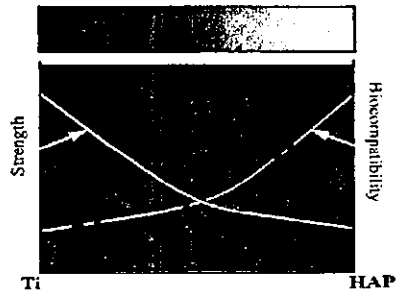

Fig. 1 Conception of FGM.

2. Materials and Methods

2.1 Preparation of FGM implant

The HAP powder which was crushed to pieces after sintered at 1150°C (SUMITOMO OSAKA CEMENT. <40 μm) and titanium nitride powder (NILACO Ltd.

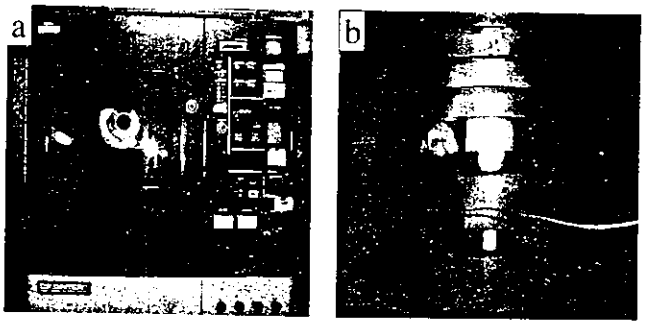

Fig. 2 a: Appearance of spark plasma sintering equipment. b: Sintering unit.

<45 μm) were blended with various ratios. These mixed powders with the different ratios of TiN and HAP were packed into the mold of ϕ20 mm × 10 mm, producing a gradient concentration from one end to the other to the depth direction. This TiN/HAP FGM was sintered under the pressure of 150 MPa at 900~1400°C by SPS. Figure 2 shows the appearance of SPS equipment. The sintered cylinder block was cut into the square rods for mechanical and animal implantation tests by the diamond disk, so that the composition gradient direction should be in the longitudinal axis.

2.2 Mechanical test

2.2.1 Brinell hardness test

The Brinell hardness test was performed in order to investigate the change of hardness in the direction of composition gradient. A steel ball with a diameter of 1.5 mm was indented under the load of 98 N for the loading time of 30 s. Three places were measured in each part of the eleven layers of gradient material, and their average was calculated.

2.2.2 Flexural test

The three point flexural test was done for the FGM rods (2 mm × 2 mm × 10 mm) with the gauge length of 10 mm and at the crosshead speed of 0.1 mm/min using the universal testing machine (INSTRON, Model 4204). Four specimens were tested and their average was calculated.

2.2.3 Compression test

The compression test was done for the FGM rods (3 mm × 3 mm × 7 mm) at the crosshead speed of 1 mm/min using the above universal testing machine. Four specimens were tested and their average was calculated.

2.3 Implantation test

Four Wister strain rats aged 14 weeks (weight 350~380 g) were used for the present experiments. After the rats were anesthetized with diethyl ether (Wako Pure Chemical Industries, Osaka Japan), pentobarbital sodium (30 mg/kg; EMBUTAL INJECTION, Dainabot, Osaka, Japan) was injected into the abdominal cavity of the rats. A hole was carefully made in the lateral surface of the diaphysis of femur using a dental round bur (ϕ1 mm), with a physiological saline external coolant, and the TiN/HAP FGM (1 mm × 1 mm × 7 mm) were inserted into bone marrow. The wound was then sutured. These rats were sacrificed at either the second or eighth week after implantation, and the tissue block involving specimens were resected. They were fixed in 10% neutral buffered formalin, washed, stained with Villanueva bone stain, and embedded in PMMA. After the tissue blocks were sectioned at 400 μm with a precision sawing machine (ISOMET 2000, BUEHLER, IL, USA), the thinner sections of about 100 μm in thickness were prepared by mechanical polishing.

2.4 Observation and analysis

Both FGM before implantation and in the tissue blocks involving specimens after implantation were observed and analyzed by optical microscopy (VANOX-S, OLYMPUS, Tokyo, Japan), SEM (HITACHI, S-2380N), electron probe micro analyzer (EPMA: JEOL JXA-8900M), and X-ray scanning analytical microscopy (XSAM: HORIBA, XGT2000V), and Raman spectroscopy (Dilor-Jobin Yvon-Spex-Horiba LABRAM).

3. Results

TiN/HAP FGM was fabricated by SPS at the temperatures 900~1400°C. For 900 and 1000°C the mechanical properties were insufficient to endure the mechanical shock at cutting process. For 1300 and 1400°C, the occurred after sintering, which was considered due to the decomposition of HAP.[15] The stable TiN/HAP FGM was obtained at 1100 and 1200°C.

Figure 3 shows the SEM observation of TiN/HAP sintered at 1100°C, the whole view (upper) and enlarged photographs of these parts (a: TiN b: 20HAP c: 80HAP d: 100HAP). The image of the part at high concentration of TiN (a, b) showed the porous structure and inadequate sintering. Sintering in the part at high concentration of HAP (c, d) was relatively more advanced and produced the condense structure.

Figure 4 shows the SEM observation of TiN/HAP sintered at 1200°C, the whole view and enlarged photographs of these parts (a: TiN b: 20HAP c: 80HAP d: 100HAP). Compared with the FGM sintered at 1100°C, sintering was advanced in each composition, although the sintering of 100%TiN region was still inadequate.

Figure 5 shows the Raman spectrum from 100%HAP region. The peak appeared near 3550 cm^{-1} is attributed to OH^-, which does not always appear in HAP. It suggests the attainment of good crystallinity.

Figure 6 shows the elemental mapping of TiN/HAP FGM by EPMA. Since Ca and P, the elements constituting HAP, show the same manner of distribution, it is suggested that HAP was not decomposed. It was also noted that Ti and N were similarly distributed in gradient and inversely to Ca and P in concentration, which proves the successfully prepared graded structure.

Figure 7 shows the Brinell hardness in each part of TiN/HAP FGM. The Brinell hardness was around 60, nearly uniform for the whole range of composition. There was not much difference between the FGM sintered at 1100 and 1200°C.

Figure 8 shows the flexural strength of TiN/HAP FGM. Flexural strength of the FGM sintered at 1100°C and 1200°C showed 65.4 MPa and 71.3 MPa, respectively. They were around the same level as a bone. The FGM fabricated at 900, 1000, 1300, and 1400°C was collapsed after sintering.

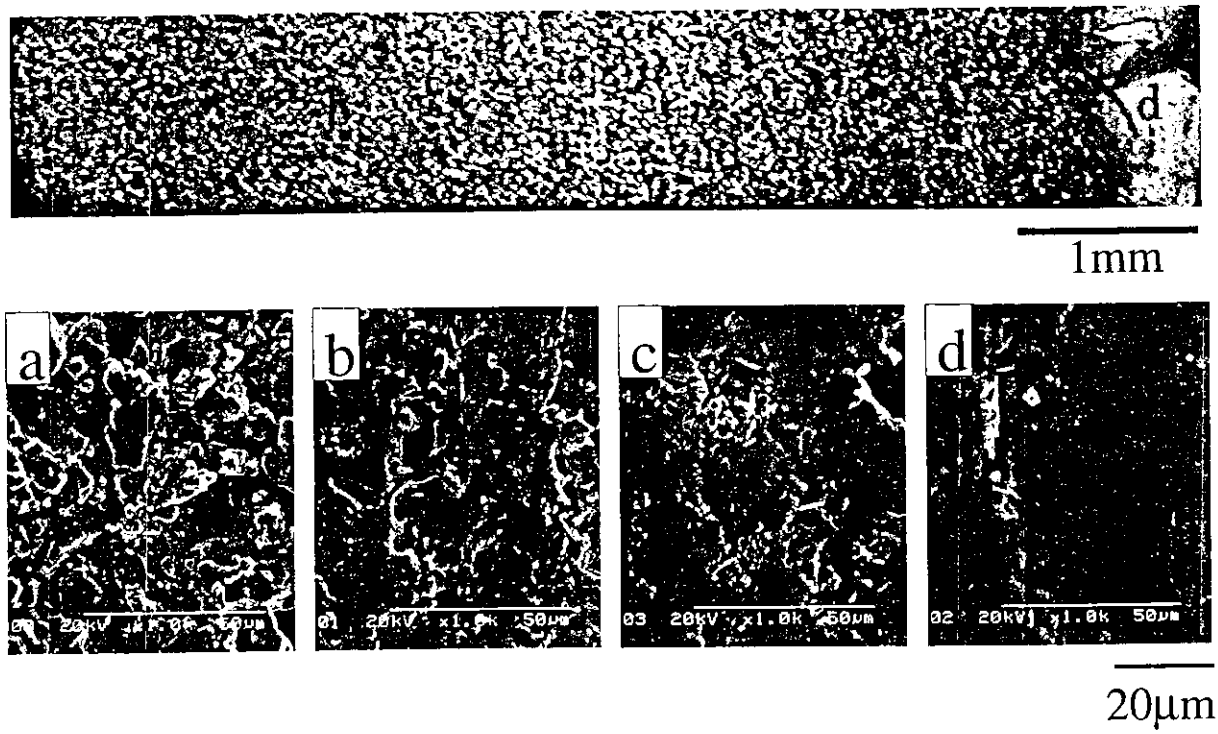

Fig. 3 SEM observation of TiN/HAP sintered at 1100°C. Whole view and enlarged photographs. a: TiN b: 20HAP c: 80HAP d: 100HAP.

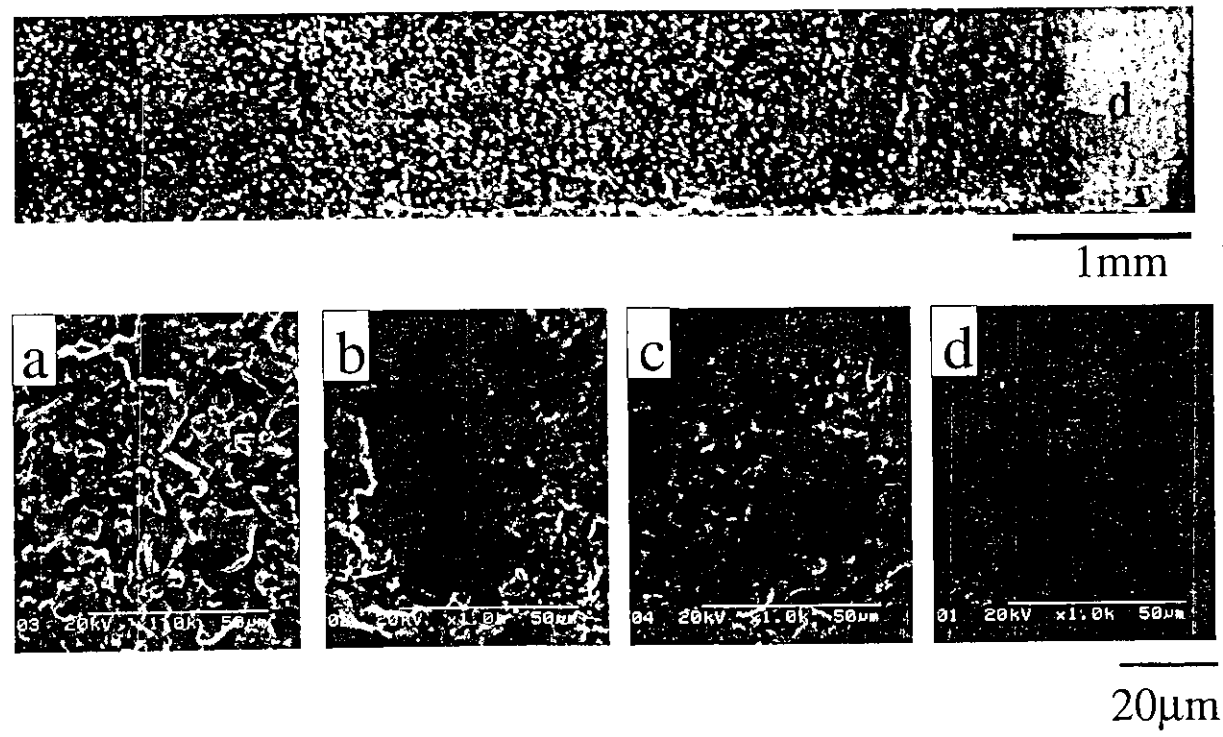

Fig. 4 SEM observation of TiN/HAP sintered at 1200°C. Whole view and enlarged photographs. a: TiN b: 20HAP c: 80HAP d: 100HAP.

Figure 9 shows the compression strength of TiN/HAP FGM. Both FGM showed the value larger than 100 MPa. The FGM fabricated at 900, 1000, 1300, and 1400°C was collapsed after sintering.

Figure 10 shows the light microscopic view of TiN/HAP implanted in the diaphysis of femur for 8 weeks in the transmission mode. Left side is 100%Ti and right side is 100%HAP regions. The cracks in 100%HAP were formed when the specimens were cut into slices for observation. The new bone was formed around FGM implant.

Figure 11 shows the enlarged views of newly formed bone in the regions of 90%TiN-10%HAP (a, c) and the 10%TiN-90%HAP (b, d) of TiN/HAP FGM after 2 and 8 weeks. The upper figures (a, b) show the newly formed bone around TiN/

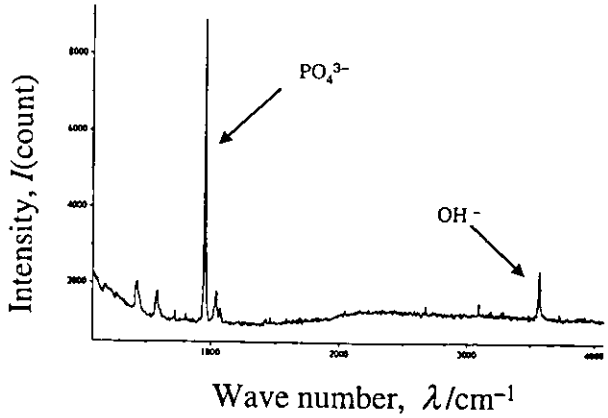

Fig. 5 Raman spectrum from 100%HAP region.

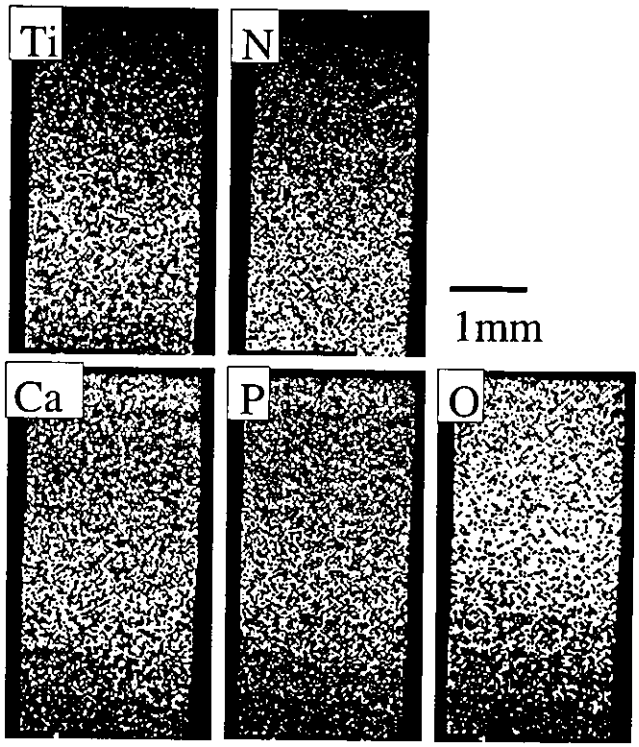

Fig. 6 EPMA elemental mapping of TiN/HAP FGM.

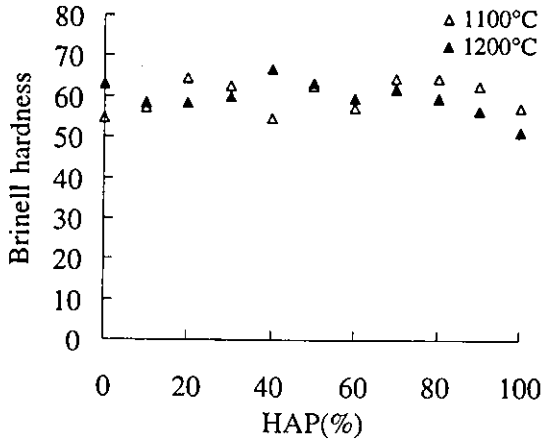

Fig. 7 Brinell hardness in each part of TiN/HAP FGM.

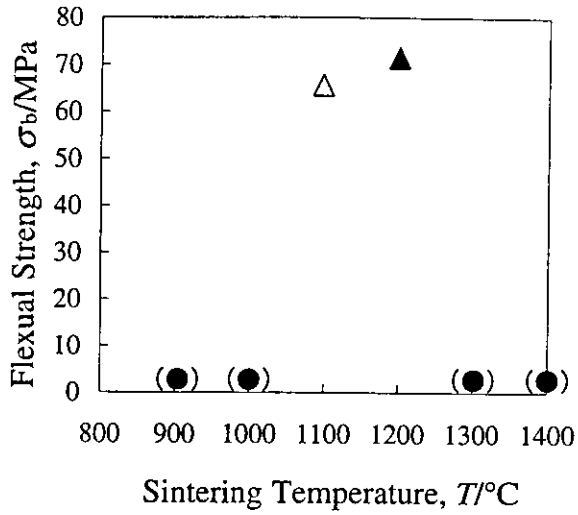

Fig. 8 Flexural strength of TiN/HAP FGM. (●): shows the auto-destructed specimens.

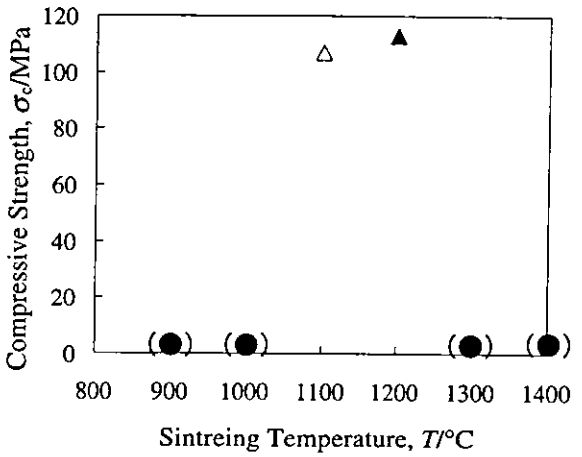

Fig. 9 Compression strength of TiN/HAP FGM. (●): shows the auto-destructed specimens.

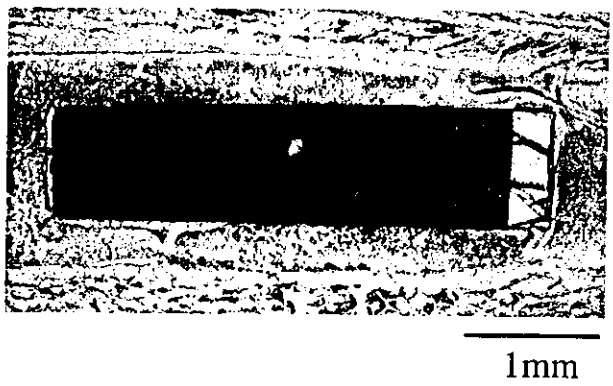

Fig. 10 Optical microscopic view of TiN/HAP FGM implant in diaphysis of femur after 8 weeks. (left: TiN, right: HAP).

HAP FGM after 2 week implantation, and the lower figures (c, d) show those after 8 weeks. In 2 weeks, an immature newly formed bone was observed around the TiN/HAP FGM. In 8 weeks, the newly formed bone around the

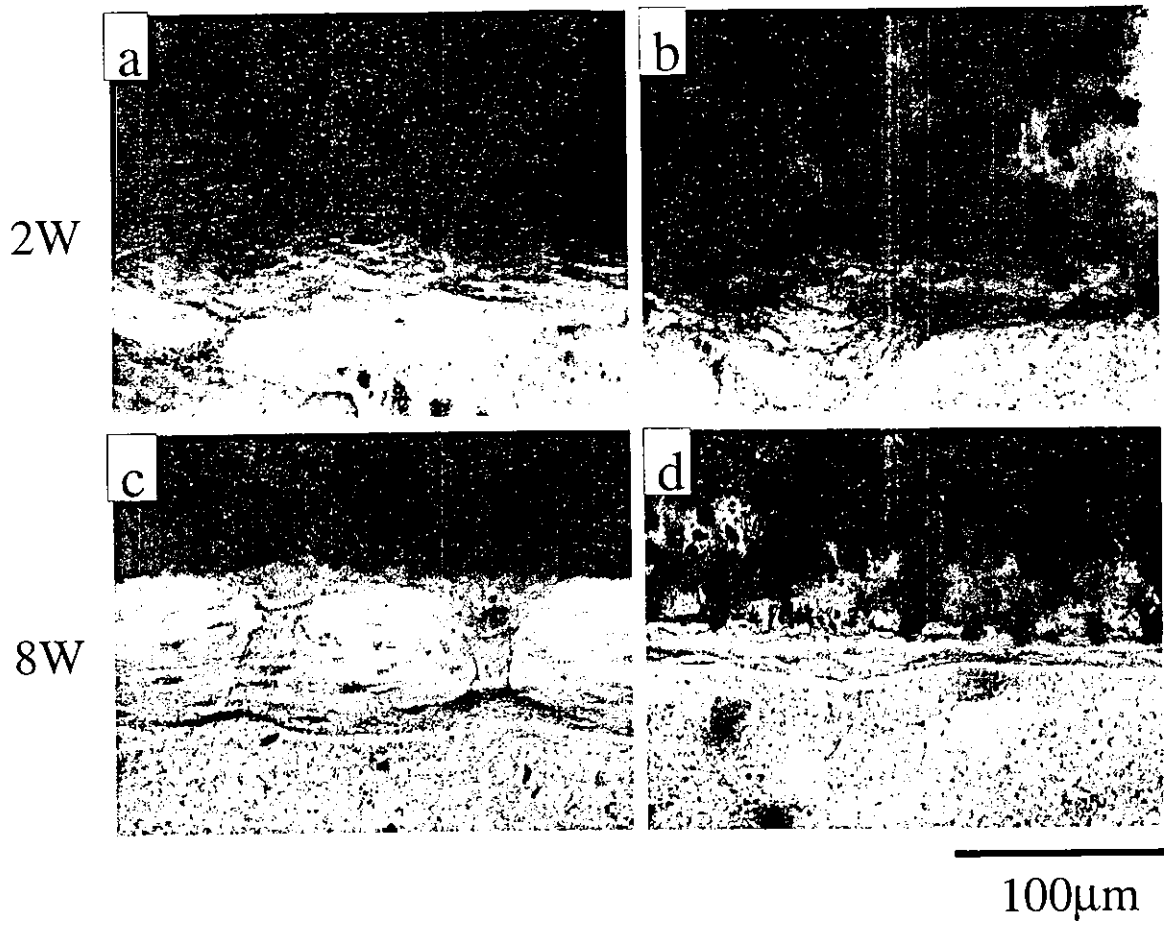

Fig. 11 Optical microscopic views of newly formed bone around TiN/HAP, after 2 weeks (a: HAP10 b: HAP90) and 8 weeks (c: HAP10 d: HAP90).

specimen was more matured. The thin lamilar structure was observed in a newly bone around the HAP rich region due to the bone remodeling (d), which was not observed at the Ti rich region (c). Very little inflammation was observed throughout the implantation period of 2 and 8 weeks.

Figure 12 shows the EPMA elemental mapping (Ca and Ti) of newly formed bone around TiN/HAP FGM after 8 week implantation. Inside the implant, Ca and Ti showed the gradient composition, complementary each other. The mapping of Ca, bone composition element, represents the formation of new bone around TiN/HAP FGM.

4. Discussion

4.1 Effect of SPS

The implant of simple substance, for example, HAP shows the high bone conduction.[1–3] However, there is a danger of fracture due to its brittle properties as dental implant when occlusal force is imposed. Ti implant has enough reliable mechanical properties. However, it takes more time until the formation of new bone after implantation, since bone conduction is inferior to HAP. In FGM which satisfies both bone conductivity and mechanical properties, it would be possible to lead a new bone to contact directly to implant material and to maturate from an early stage in root. In this study, TiN/HAP FGM was successfully fabricated by SPS.

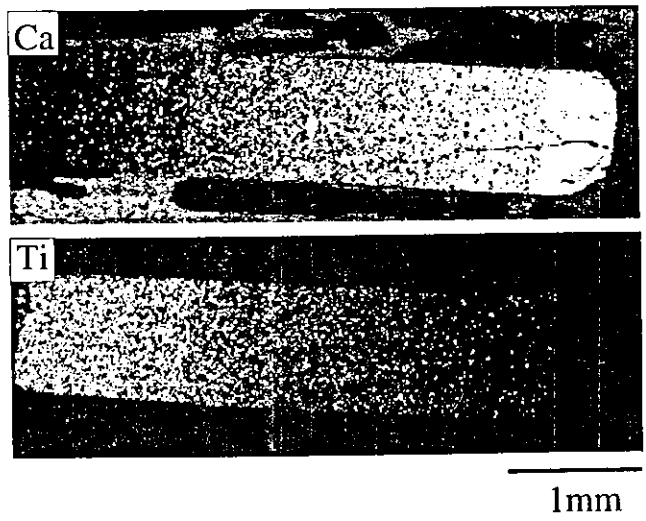

Fig. 12 EPMA elemental mapping of new bone formation around TiN/HAP inserted in diaphysis of femur for 2 weeks.

FGM is produced by intermingling two or more kinds of metals, ceramics or polymers. The optimal sintering conditions are usually different for these components and the formation of simultaneous sintering is difficult. SPS can promote the efficient and uniform sintering by generating

spark plasma between particles. This differs greatly from the conventional sintering using an electric furnace. Fabrication of stable Ti/HAP system FGM was limited up to Ti/Ti30%HAP, since heating at 1300°C was necessary to make sintering by electric furnace heating and FGM for lager content of HAP such as Ti/100%HAP was not possible.[13] By use of SPS, heating temperature could be lowered due to the enhancement of sintering and it was possible to fabricate Ti/100%HAP.[13-16] When pure Ti was used for FGM by SPS, 750°C was inadequate for sintering of Ti/HAP, but the self-destruction occurred after sintering at 900°C and 1000°C due to the decomposition of HAP.[15] The compromising optimum sintering temperature was found as 850°C.[15] When TiN was used for TiN/HAP FGM, the temperature of 900 and 1000°C was insufficient to endure to the mechanical shock at cutting. At 1300 and 1400°C, the self-destruction of specimens occurred after sintering, which was considered due to the decomposition of HAP. The sintering temperature was thus set as 1100 and 1200°C.

4.2 Mechanical properties of FGM

Since the composition and structure are changed from part to part in FGM, evaluation of their properties is not simple, compared with the homogeneous material. The Brinell hardness test evaluates the hardness in each part of FGM. Compression and flexural tests evaluate the representive value of mechanical strength for the whole sample. Brinell hardness test is suitable to evaluate a complex with porosity which can be measured from the depth of indentation using a spherical steel ball as indented. The hardness of TiN was very high (Hv~1300) nearly ten times of Ti.[19,20] In TiN region, sintering was inadequate and porous structure was observed by SEM (Figs. 3, 4). This resulted in the uniform Brinell hardness for the whole range in spite of the gradient composition from TiN to HAP.

The specimens sintered at 1100 and 1200°C had the flexural and compression strength of the similar level as a bone. Both strengths are slightly more improved for 1200°C than 1100°C, although the hardness of each part is nearly the same for the FGM sintered at 1100 and 1200°C. The results of compression and flexural tests for FGM are very much affected by existence of weak part. Since the mechanical properties of FGM are not uniform, fracture tends to initiate from crack formation at the weakest part, usually in the part of high ceramic content where sintering is insufficient, porosity is high and brittleness is predominant. Therefore the results of compression and flexural tests are not necessarily consistent with the Brinell hardness test. The most influential part for strength for the whole specimen is the degree of insufficient sintering in the TiN rich part, since 1100~1200°C is still insufficient for sintering of TiN whose melting point is 2950°C. The sintering at 1200°C improved the strength of TiN part, which thus resulted in the increase of compression and flexural strength compared with that of 1100°C.

4.3 Bone conductivity

Ti and HAP are widely used in clinics, because of high biocompatibility and bone conductivity. The chemically stable properties of TiN, especially the excellent corrosion resistance which may be better than Ti, would contribute to its biocompatibility.[17-20] Our previous study of implantation tests in the soft and hard tissue showed that TiN has the nearly equivalent biocompatibility as Ti and is suitable for the abrasion resistant implant which may be used for the abutment part of dental implant and the sliding part of artificial joint.[19,20]

In this study, the implantation experiment was conducted to observe the difference of the bone formation capability in each part of FGM. The rat femur was used for the implantation test since it is the largest space in rat for hard tissue which can hold a long specimen to compare the reaction for the composition from TiN to HAP in the longitudinal direction under nearly the same conditions. No inflammation was histopathologically observed on the surrounding of FGM in two and eight weeks after the direction and suture for implantation. EPMA elemental mapping was also performed for the analysis of hard tissue, where new bone formation was clearly recognized for the whole part around implant in Ca mapping. Theses confirmed that any part of TiN/HAP has biocompatibility. The further detailed observation by optical microscopy showed that the maturation of new bone was more advanced in the HAP rich region than in the Ti rich region. This suggests that a vital reaction in hard tissue changes in inclination in accordance to the inclination structure of material.

5. Conclusions

(1) By use of TiN instead of Ti, the decomposition of HAP could be suppressed.
(2) TiN/HAP FGM could be successfully fabricated at 1100 and 1200°C by SPS.
(3) The Brinell hardness was around 60, nearly uniform for the whole range of composition.
(4) Flexural strength of TiN/HAP FGM sintered at 1100°C and 1200°C showed 65.4 MPa and 71.3 MPa respectively, and compression strength of TiN/HAP FGM showed more than 100 MPa.
(5) The new bone was formed directly on the implants. No inflammation was observed throughout the implantation period of 2~8 weeks.
(6) In 8 weeks, the maturation of newly formed bone was more advanced in the HAP rich region.
(7) The sintering of TiN rich part was still insufficient for the temperature up to 1200°C.

Acknowledgements

Research was performed under Grant-in-Aid for Scientific Research (B) (2) from the Ministry of Education, Science, Sports and Culture of Japan, and Health and Laybour Sciences Research Grants in Research on Advanced Medical Technology from the Ministry of Health, Laybour and Welfare of Japan. The authors are grateful to Dr. Koichi OMAMYUDA of SUMITOMO OSAKA CEMENT for the supply of HAP.

REFERENCES

1) F. C. M. Driessens and R. M. H. Verbeeck: *Biominerals*, (CRC Press, Boca Raton, 1990) pp. 1.
2) H. Aoki: *Science and medical application of hydroxyapatite*, (Inc. Ishiyaku, Euro. America. Tokyo, 1994) pp. 1.
3) H. Aoki: *Medical applications of hydroxyapatite*, (Jap. Asso. Apatite. Science. Tokyo, 1991) pp. 1.
4) T. Hirai: *Materials Science and Technology. Processing of Ceramics Part 2*, vol. 17B, ed. by R. W. Cahn, P. Haasen and E. J. Kramer, (Weinheim, Verlagsgesellschaft, 1996) pp. 293–341.
5) F. Watari, A. Yokoyama, F. Saso, M. Uo and T. Kawasaki: *Functionally Graded Materials 1996*, ed. by I. Shiota Y. Miyamoto, (Elsevier, Amsterdam, 1997) pp. 749–754.
6) F. Watari, A. Yokoyama, F. Saso, M. Uo and T. Kawasaki: Composites Part B **28B** (1997) 5–11.
7) F. Watari, A. Yokoyama, F. Saso, M. Uo, H. Matsuno and T. Kawasaki: J. Japan Inst. Metals **62** (1998) 1095–1101. (in Japanese).
8) F. Watari, A. Yokoyama, F. Saso, M. Uo, H. Matsuno and T. Kawasaki: *Functionally Graded Materials 1998*, ed. by W. A. Kayser, (Trans Tech Publications, Zurich, 1999) pp. 356–361.
9) H. Takahashi, F. Watari, F. Nishimura and H. Nakamura: Dent. Mater. J. **11** (1992) 462–468.
10) F. Watari, A. Yokoyama, H. Matsuno, R. Miyao, M. Uo, Y. Tamura, T. Kawasaki, M. Omori and T. Hirai: *Functionally Graded Materials 2000, Ceramic Transaction 114*, ed. by K. Trumble, K. Bowman, I. Reimanis, S. Sampath, (Am. Ceramic Soc., 2001) pp. 73–80.
11) F. Watari, A. Yokoyama, H. Matsuno, R. Miyao, M. Uo, T. Kawasaki, M. Omori and T. Hirai: *Functionally Graded Materials in the 21st Century*, ed. by K. Ichikawa, (A Workshop on Trends and Forecasts, Kluwer Academic Publishers, Boston, 2001) pp. 187–190.
12) H. Takahashi: Dent. Mater. J. **12** (1993) 595–612.
13) F. Watari, A. Yokoyama, F. Saso, M. Uo and T. Kawasaki: *Proc. 3rd Int. Symp. Structural & Functionally Gradient Materials*, ed. by B. Ilschner, N. Cherradi, (Polytechniques Press, Romandes, Lausanne, 1995) pp. 703–708.
14) F. Watari, M. Omori, T. Hirai, A. Yokoyama, H. Matsuno, M. Uo, R. Miyao, Y. Tamura and T. Kawasaki: J. Jpn. Soc. Powder & Powder Metallurgy **47** (2000) 1226–1233.
15) R. Miyao, A. Yokoyama, F. Watari and T. Kawasaki: J. Jpn. Soc. Dent. Mater and Devices **20** (2001) 344–355. (in Japanese).
16) F. Watari, A. Yokoyama M. Omori, T. Hirai, H. Kondo, M. Uo and T. Kawasaki: Compos. Sci. Tech. **64** (2004) 893–908.
17) H. Matsuno, A. Yokoyama, F. Watari, M. Uo and T. Kawasaki: J. Jpn. Soc. Dent. Mater and Devices **8** (1999) 447–462. (in Japanese).
18) H. Matsuno, A. Yokoyama, F. Watari, M. Uo and T. Kawasaki: Biomaterials **22** (2001) 1253–1262.
19) Y. Tamura, A. Yokoyama, F. Watari and T. Kawasaki: Dent. Mater. J. **21** (2002) 355–372.
20) Y. Tamura, A. Yokoyama, F. Watari, M. Uo and T. Kawasaki: Mater. Trans. **43** (2002) 3043–3051.